

Tuning the Excited-State Properties of Platinum(II) Diimine Dithiolate Complexes

Scott D. Cummings and Richard Eisenberg*

Contribution from the Department of Chemistry, University of Rochester, Rochester, New York 14627

Received April 26, 1995. Revised Manuscript Received October 26, 1995[⊗]

Abstract: Two series of Pt(diimine)(dithiolate) complexes have been prepared in order to investigate the effects of molecular design on the excited-state properties of this chromophore. The first series comprises Pt(dbbpy)(dithiolate) complexes where dbbpy = 4,4'-di-*tert*-butyl-2,2'-bipyridine and the dithiolates are 1-(*tert*-butylcarboxy)-1-cyanoethylene-2,2-dithiolate (tbcda), 1-diethylphosphonate-1-cyanoethylene-2,2-dithiolate (cpdt), 6,7-dimethylquinoxaline-2,3-dithiolate (dmqdt), maleonitriledithiolate (mnt), and toluene-3,4-dithiolate (tdt). The second series comprises Pt(diimine)(tdt) complexes where the diimines are 3,4,7,8-tetramethyl-1,10-phenanthroline (tmphen), 4,4'-di-*tert*-butyl-2,2'-bipyridine (dbbpy), 4,4'-dimethyl-2,2'-bipyridine (dmbpy), 2,2'-bipyridine (bpy), 1,10-phenanthroline (phen), 5-chloro-1,10-phenanthroline (Cl-phen), 4,4'-dichloro-2,2'-bipyridine (Cl₂bpy), and 4,4'-bis(ethoxycarbonyl)-2,2'-bipyridine (EC-bpy). All of the compounds display solvatochromic absorption bands and solution luminescence, which are attributed to a common charge-transfer-to-diimine excited state. The excited-state energies can be tuned by approximately 1 eV through ligand variation. Solution lifetimes range from 1 ns to over 1000 ns and Φ_{em} range from 6.4×10^{-3} to less than 10^{-5} in CH₂Cl₂. Based on these data, the nonradiative and radiative decay rate constants have been calculated. For the Pt(diimine)(tdt) series, the nonradiative decay rate constants increase exponentially with decreasing energy, in agreement with the Energy Gap Law, while those for the Pt(dbbpy)(dithiolate) complexes do not exhibit a similar correlation. Excited-state redox potentials have been estimated for all of the complexes from spectroscopic and electrochemical data. The ability to tune the driving force for bimolecular excited-state electron-transfer reactions has been demonstrated for eight of the complexes using reductive and oxidative quenching experiments.

Introduction

Research involving the excited-state processes of transition metal diimine complexes has dominated the field of inorganic photochemistry for the past two decades.¹ Growth in this area has been driven by rapid advances in the techniques of studying excited-state transient species and in the theory of photoinduced electron transfer. Further support has come from promising results concerning the use of metal diimine chromophores in applications such as solar energy conversion, supramolecular assemblies, photocatalysis, nonlinear optics, photonic molecular devices, and photoluminescent probes of biological systems.^{2–7} Research continues to focus on transition metal diimine complexes because they often possess long-lived excited states capable of bimolecular energy and electron transfer as well as efficient photoluminescence. Synthetic strategies are aimed at preparing complexes having a high degree of stability and having excited-state properties that can be controlled by systematic variation in molecular structure. These properties, which classical coordination compounds and organometallic complexes often lack, are crucial to most potential applications.

An extensive amount of work has involved the homoleptic Ru(II) tris-diimine complex Ru(bpy)₃²⁺ and its derivatives as well as related complexes of Fe(II) and Os(II). Other d⁶ octahedral complexes having chelating diimines that have received much attention include Re(I) diimine carbonyl complexes such as the prototypical Re(CO)₃Cl(diimine) system and Rh(III) and Ir(III) bis- and tris-chelating diimine systems. In contrast, relatively little work has been done using Pt(II) metal complexes. Much of the early studies involved complexes such as PtX₄²⁻ (X = halide), Pt(diimine)X₂, and Pt(diimine)₂²⁺, for which emission was observed only in frozen solvent glasses or in the solid state.^{8,9} Recently, a number of square-planar Pt(II) complexes, most of which contain α,α' -diimine or related pyridyl chelates, have been prepared that display long-lived solution luminescence in ambient conditions. One of the first examples of this group was Pt(2-thienylpyridine)₂, which contains cyclometalated thienylpyridyl chelating ligands.¹⁰ Commencing in 1989, we have reported an extensive series of solution luminescent Pt(diimine) complexes that contain 1,1- and 1,2-dithiolate ligands.¹¹ In addition to these complexes, solution-luminescent Pt(II) complexes of the type Pt(diimine)-LL have been reported for which L is phenyl,¹² phenylacetyl-ide,¹³ and CN,¹³ and LL is chelating phosphine¹³ or biphenyl

[⊗] Abstract published in *Advance ACS Abstracts*, January 15, 1996.

(1) Balzani, V.; Moggi, L. *Coord. Chem. Rev.* **1990**, *97*, 313.

(2) Meyer, T. J. *Acc. Chem. Res.* **1989**, *22*, 163–170.

(3) Balzani, V.; Scandola, F. *Supramolecular Photochemistry*; Ellis Horwood: Chichester, UK, 1991.

(4) Pelizzetti, E.; Serpone, N. *Homogeneous and Heterogeneous Photocatalysis*; Pelizzetti, E., Serpone, N., Ed.; D. Reidel Publishing: Dordrecht, Holland, 1985.

(5) Cheng, L.-T.; Tam, W.; Eaton, D. F. *Organometallics* **1990**, *9*, 2856–2857.

(6) Prasad, P. N.; Reinhardt, B. A. *Chem. Mater.* **1990**, *2*, 660–669.

(7) Friedman, A. E.; Chambron, J.-C.; Sauvage, J.-P.; Turro, N. J.; Barton, J. K. *J. Am. Chem. Soc.* **1990**, *112*, 4960.

(8) Camassei, F. D.; Ancarani-Rossiello, L.; Castelli, F. *J. Luminescence* **1973**, *8*, 71–81.

(9) Webb, D. L.; Rossiello, L. A. *Inorg. Chem.* **1971**, *10*, 2213–2218.

(10) Barigelletti, F.; Sandrini, D.; Maestri, M.; Balzani, V.; von Zelewsky, A.; Chassot, L.; Joliet, P.; Maeder, U. *Inorg. Chem.* **1988**, *27*, 3644–3647.

(11) Zuleta, J. A.; Chesta, C. A.; Eisenberg, R. *J. Am. Chem. Soc.* **1989**, *111*, 8916–8917.

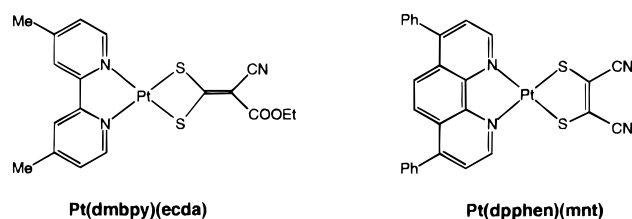
(12) Vogler, C.; Schwederski, B.; Klein, A.; Kaim, W. *J. Organomet. Chem.* **1992**, *436*, 367–378.

(13) Vogler, C.; Schwederski, B.; Klein, A.; Kaim, W. *J. Organomet. Chem.* **1992**, *436*, 367–378.

ligands.^{14,15} Solution luminescence has also been observed for Pt(II) complexes having larger heteroaromatic chelates, including cyclometalated Pt(2,9-diphenylphenanthroline)L (L = CH₃-CN, substituted pyridines),¹⁶ Pt(terpy)X⁺ (terpy = 2,2':6',2''-terpyridine; X = Cl, NCS, OMe, OH),¹⁷ and Pt(pQP)²⁺ (pQP = 3'',5,5',5'''-tetramethyl-2,2':6',2'':6'',2'''-quaterpyridine) complexes.¹⁸ The heteroaromatic ligands each have low-energy π^* orbitals that are involved in charge-transfer (CT) excited states of their respective complexes. For these complexes, the luminescent excited states can involve a variety of orbitals. Intraligand charge-transfer (ILCT), metal-to-ligand charge-transfer (MLCT), charge-transfer-to-diimine, and ligand-to-ligand charge-transfer (LLCT) excited states have been reported. In these examples, the highest occupied molecular orbital (HOMO) may have orbital contributions from the metal ion, the polypyridyl moiety, the other ligands in the complex and/or mixtures thereof, but the lowest unoccupied molecular orbital (LUMO) in each case is localized on the heteroaromatic chelating ligand.

The Pt(II) diimine complexes that have been reported in the literature display a wide variety of excited-state lifetimes, ranging from immeasurably short up to several μ seconds in fluid solution. Proposals regarding the ability to control these lifetimes usually focus on radiationless deactivation of the emissive CT state by energetically-close metal-centered (MC) d-d states. A few complexes appear to support this proposal, displaying longer lifetimes as the emitting state is lowered in energy away from the MC state via ligand substitution.^{10,17} The effect that further lowering of the emission energy has on excited-state lifetime in these complexes has not been explored systematically since emission maxima for monomeric Pt(II) chromophores in solution rarely lie below 17 000 cm⁻¹.¹⁷ Very few complexes have been examined for calculations of excited-state redox potentials or for electron-transfer quenching, and there has been no systematic study of how to tune the excited-state properties of Pt(II) chromophores for a large series of complexes.

Our laboratory has focused on studying Pt(diimine)(dithiolate) complexes in order to determine the full range of excited-state properties for this chromophore. The first examples of solution luminescence from a Pt(diimine)(dithiolate) complex were from the complexes Pt(dmbpy)(ecda) and Pt(dpphen)(mnt), where dmbpy = 4,4'-dimethyl-2,2'-bipyridine, ecda = 1-(ethoxycarbonyl)-1-cyanoethylene-2,2-dithiolate, dpphen = 4,7-diphenyl-1,10-phenanthroline, and mnt = maleonitriledithiolate.¹¹ The synthesis of new types of Pt(diimine)(dithiolate) complexes



and spectroscopic study of their CT energies, temperature-

(13) Chan, C.-W.; Cheng, L.-K.; Che, C.-M. *Coord. Chem. Rev.* **1994**, *132*, 87-97.

(14) Blanton, C. B.; Murtaza, Z.; Shaver, R. J.; Rillema, D. P. *Inorg. Chem.* **1992**, *31*, 3230-3235.

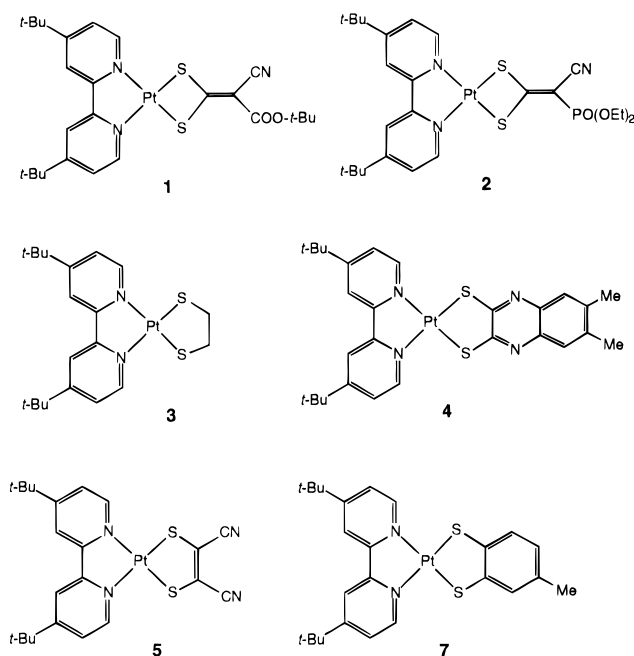
(15) Maestri, M.; Sandrini, D.; Balzani, V.; von Zelewsky, A.; Deuschel-Cornioley, C.; Jolliet, P. *Helv. Chim. Acta* **1988**, *71*, 1053-1059.

(16) Chan, C.-W.; Lai, T. F.; Che, C.-M.; Peng, S.-M. *J. Am. Chem. Soc.* **1993**, *115*, 11245.

(17) Aldridge, T. K.; Stacy, E. M.; McMillin, D. R. *Inorg. Chem.* **1994**, *33*, 722-727.

(18) Chan, C.-W.; Che, C.-M.; Cheng, M.-C.; Wang, Y. *Inorg. Chem.* **1992**, *31*, 4874-4878.

Chart 1



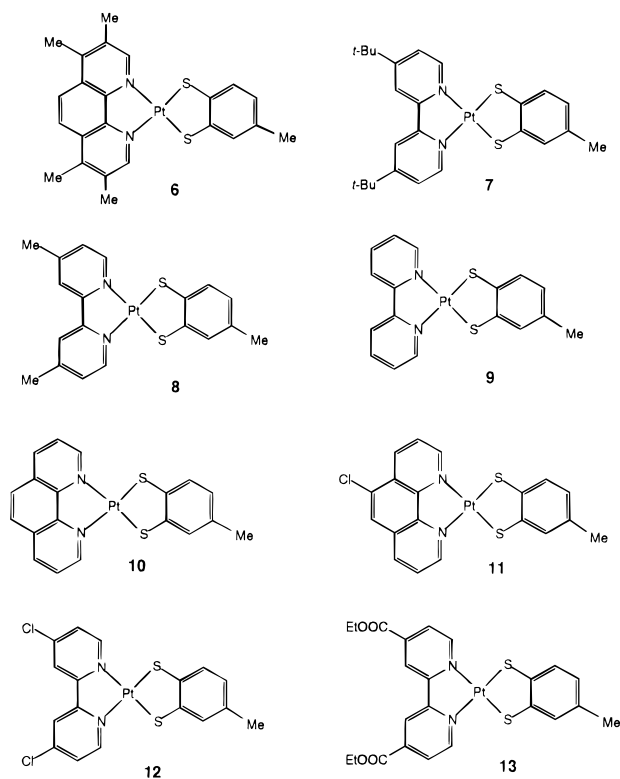
dependent emission behavior, and electronic structure led to assignment of the lowest-energy excited states of these complexes.¹⁹ For most of them, the excited state involves a HOMO which is a mixture of Pt(d) and dithiolate orbital character and a LUMO which is a π^* orbital of the diimine and has been termed charge-transfer-to-diimine. A charge-transfer-to-dithiolate excited state, which involves the same HOMO and a LUMO which is a π^* dithiolate orbital, appears to lie in close proximity and, for a few of the complexes, lower in energy.²⁰ Solution lifetime measurements were carried out on complexes having sufficient solubility and yielded values ranging from 3 to 25 ns in dichloromethane. Excited-state reduction potentials were estimated for several complexes and ranged from 0.96-1.15 V vs SCE. Important goals for the further development of this chromophore have included increasing the lifetimes and excited-state redox potentials, improving both solubility and stability characteristics of the complexes, and understanding what structural factors influence the excited-state properties of these systems.

In the present study, we describe the synthesis, characterization, and photoluminescent properties of two series of Pt-(diimine)(dithiolate) complexes for which the chelating ligands have been systematically varied. The first series, shown in Chart 1, comprises Pt(dbpy)(dithiolate) complexes for which dbpy = 4,4'-di-*tert*-butyl-2,2'-bipyridine and the dithiolates are a variety of 1,1- and 1,2-dithiolate chelating ligands. In the second series, shown in Chart 2, the 2,2'-bipyridine and 1,10-phenanthroline ligands are modified with electron-donating and electron-accepting substituents, and the dithiolate is held constant as 3,4-toluenedithiolate (tdt). The purpose of this study is to determine whether the excited-state properties of the Pt-(diimine)(dithiolate) chromophore can be controlled through variation in the molecular design. Specific properties which are of interest are the charge-transfer absorption and emission energies, emission quantum yields, lifetimes, excited-state redox potentials, and bimolecular electron-transfer rate constants.

(19) Zuleta, J. A.; Bevilacqua, J. M.; Rehm, J. M.; Eisenberg, R. *Inorg. Chem.* **1992**, *31*, 1332.

(20) Zuleta, J. A.; Bevilacqua, J. M.; Proserpio, D. M.; Harvey, P. D.; Eisenberg, R. *Inorg. Chem.* **1992**, *31*, 2396.

Chart 2



Experimental Section

Chemicals. The diimines 2,2'-bipyridine (bpy), 1,10-phenanthroline (phen), 4,4'-dimethyl-2,2'-bipyridine (dmbpy), 3,4,7,8-tetramethyl-1,10-phenanthroline (tmphen), and 5-chloro-1,10-phenanthroline (Cl-phen) were used as received from Aldrich. The diimines 4,4'-bis(ethoxycarbonyl)-2,2'-bipyridine (EC-bpy), 4,4'-di-*tert*-butyl-2,2'-bipyridine (dbbpy), and 4,4'-dichloro-2,2'-bipyridine (Cl₂bpy) were prepared according to literature methods.^{21–23} The dithiolates 1-(*tert*-butylcarboxy)-1-cyanoethylene-2,2-dithiolate (K₂tbcd), 1-diethylphosphonate-1-cyanoethylene-2,2-dithiolate (K₂cpdt), 6,7-dimethyl-quinoxaline-2,3-dithiolate (K₂dmqdt), and maleonitriledithiolate (Na₂mnt) were prepared following literature methods.^{24–26}

3,4-Toluenedithiol (H₂tdt) and 1,2-ethanedithiol were used as received from Aldrich, and K₂PtCl₄ was used as received from Alfa/AESAR Johnson-Matthey. *N,N*-Dimethylaniline (99.5+%) and nitrobenzene (99+%) were degassed but otherwise used as received from Aldrich. *N,N,N,N*-Tetramethylbenzidine, *N,N,N,N*-tetramethyl-1,4-phenylenediamine, *p*-nitrobenzaldehyde, and *p*-dinitrobenzene were purchased from Aldrich and purified by sublimation and handled under nitrogen. Dichloromethane was dried with CaH₂ and distilled prior to use. Other solvents used for spectroscopy were purified using standard methods.²⁷

Synthesis of Pt(diimine)(dithiolate) Complexes. The Pt(diimine)-(dithiolate) complexes were prepared by displacement of the two chlorides in the corresponding Pt(diimine)Cl₂ precursor with the appropriate dithiolate chelating ligand. The Pt(diimine)Cl₂ complexes were prepared by the method of Rund by heating a mixture of the diimine suspended in a solution of 1 equiv of K₂PtCl₄ in H₂O with 1 drop of HCl until the water solution was colorless (0.5–5 h).²⁸ Several

of the Pt(diimine)Cl₂ complexes have been prepared previously, while others are new.

Pt(tmphen)Cl₂: ¹H NMR (DMSO-*d*₆) δ 9.02 (2 H, s), 8.40 (2 H, s), 2.81 (6H, s), 2.60 (6H, s).

Pt(dmbpy)Cl₂: ¹H NMR (DMSO-*d*₆) δ 9.34 (2 H, d, *J* = 5.6 Hz), 8.58 (2H, s), 7.83 (2 H, d, *J* = 5.2 Hz), 1.41 (18 H, s).

Pt(dmbpy)Cl₂: ¹H NMR (DMSO-*d*₆) δ 9.23 (2 H, d, *J* = 5.8 Hz), 8.42 (2H, s), 7.64 (2 H, d, *J* = 5.8 Hz), 2.47 (6 H, s).

Pt(bpy)Cl₂: ¹H NMR (DMSO-*d*₆) δ 9.48 (2 H, d, *J* = 6 Hz), 8.59 (2H, d, *J* = 8 Hz), 8.40 (2 H, d, *J* = 8 Hz), 7.83 (2 H, dd, *J* = 7 Hz).

Pt(phen)Cl₂: ¹H NMR (DMSO-*d*₆) δ 9.68 (2 H, d, *J* = 5 Hz), 9.03 (2H, d, *J* = 8 Hz), 8.28 (2 H, s), 8.16 (2 H, dd, *J* = 5 Hz, 8 Hz).

Pt(Cl-phen)Cl₂: ¹H NMR (DMSO-*d*₆) δ 9.77 (1 H, d, *J* = 4.8 Hz), 9.67 (1 H, d, *J* = 5.6 Hz), 9.12 (1 H, d, *J* = 8.4 Hz), 8.96 (1 H, d, *J* = 7.6 Hz), 8.63 (1 H, s), 8.26 (1 H, dd, *J* = 8.4, 5.6 Hz), 8.17 (1 H, dd, *J* = 8.4, 5.6 Hz).

Pt(Cl₂bpy)Cl₂: ¹H NMR (DMSO-*d*₆) δ 9.40 (2 H, d, *J* = 6.4 Hz), 8.92 (2H, s), 8.02 (2 H, d, *J* = 6.4 Hz).

Pt(EC-bpy)Cl₂: ¹H NMR (DMSO-*d*₆) δ 8.95 (2 H, d, *J* = 4.8 Hz), 8.84 (2 H, s), 7.94 (2 H, dd, *J* = 4.8 Hz, *J* = 1.2 Hz), 4.42 (4 H, q, *J* = 7.2 Hz), 1.36 (6 H, t, *J* = 7.2 Hz).

The Pt(diimine)(dithiolate) complexes were prepared following two literature methods with the syntheses performed under N₂ using standard inert atmosphere techniques.^{29,30}

Pt(dbbpy)(tbcd) (1). A 268.5 mg (0.5024 mmol) sample of Pt-(dbbpy)Cl₂ was placed in a round-bottom flask under N₂ and partially dissolved in a mixture of 30 mL of acetone and 15 mL of dichloromethane. To this was added a solution of 218 mg (0.7428 mmol) of K₂tbcd in methanol. A bright yellow solution formed immediately and was stirred for an additional 30 min. The solvents were removed under vacuum, and the product redissolved in dichloromethane and filtered. The filtrate was poured into cold hexanes to precipitate the bright yellow product, which was then filtered, washed several times with diethyl ether, hexanes and isopropyl alcohol/H₂O, and dried under vacuum. The yield was 97% based on Pt: ¹H NMR (DMSO-*d*₆) δ 8.70 (2 H, d, *J* = 1.6 Hz), 8.36 (2 H, dd, *J* = 6 Hz, 3.2 Hz), 7.74 (2 H, ddd, *J* = 6 Hz, 3.2 Hz, 1.6 Hz), 1.45–1.42 (two singlets, 27 H). Anal. Calcd for PtC₂₆H₃₃N₃O₂S₂: C, 46.01; H, 4.90. Found: C, 45.74; H, 4.79.

Pt(dbbpy)(cpdt) (2). This complex was prepared using the method described for Pt(dbbpy)(tbcd), using 132.5 mg of Pt(dbbpy)Cl₂ and 100 mg of K₂cpdt: 167.7 mg of a bright yellow product was isolated (95% yield based on Pt); ¹H NMR (DMSO-*d*₆) δ 8.71 (2 H, d, *J* = 1.6 Hz), 8.41 (2 H, d, *J* = 6 Hz), 7.73 (2 H, dd, *J* = 6 Hz, 2 Hz), 4.01 (4 H, q, *J* = 7.2 Hz), 1.42 (18 H, s), 1.26 (6 H, t, *J* = 7.2 Hz). Anal. Calcd for PtC₂₅H₃₄N₃O₃PS₂: C, 41.95; H, 4.93. Found: C, 41.73; H, 4.56.

Pt(dbbpy)(edt) (3). This complex was prepared using the method described for Pt(dbbpy)(tbcd) using 199.0 mg of Pt(dbbpy)Cl₂ and 0.05 mL of H₂edt and excess KOH: 112.0 mg of a red-brown product was isolated (54% yield based on Pt); ¹H NMR (CD₂Cl₂) δ 9.10 (2 H, d, *J* = 6 Hz), 7.95 (2 H, d, *J* = 2 Hz), 7.46 (2 H, dd, *J* = 6 Hz, 2 Hz), 2.34 (4 H, s), 1.42 (18 H, s). Anal. Calcd for PtC₂₆H₂₀N₂S₂: C, 43.23; H, 5.08. Found C, 43.30; H, 4.98.

Pt(dbbpy)(dmqdt) (4). This complex was prepared using the method described for Pt(dbbpy)(tbcd) using 246 mg of Pt(dbbpy)Cl₂ and 150 mg of H₂dmqdt and excess NaOH: 302.1 mg of a bright orange-red product was isolated (96% yield based on Pt); ¹H NMR (DMSO-*d*₆) δ 8.84 (2 H, d, *J* = 6 Hz), 8.72 (2 H, s), 7.89 (2 H, dd, *J* = 6 Hz, 1.6 Hz), 7.519 (2 H, s), 2.36 (6 H, s), 1.44 (18 H, s).

Pt(dbbpy)(mnt) (5). This complex was prepared using the method described for Pt(dbbpy)(tbcd) using 229.2 mg of Pt(dbbpy)Cl₂ and 98.3 mg of Na₂mnt: 176.5 mg of a red product was isolated (68% yield based on Pt); ¹H NMR (DMSO-*d*₆) δ 8.73 (2 H, d, *J* = 6.4 Hz), 8.68 (2 H, d, *J* = 2 Hz), 7.78 (2 H, dd, *J* = 6 Hz, 2 Hz), 1.43 (18 H, s). Anal. Calcd for PtC₂₂H₂₄N₄S₂: C, 43.77; H, 4.01. Found C, 43.75; H, 3.83.

(29) Zuleta, J. A.; Burberry, M. S.; Eisenberg, R. *Coord. Chem. Rev.* **1990**, *97*, 47–64.

(30) Kumar, L.; Puthraya, K. H.; Srivastava, T. S. *Inorg. Chim. Acta* **1984**, *86*, 173–178.

(21) Elliott, C. M.; Hershenhart, E. J. *J. Am. Chem. Soc.* **1982**, *104*, 7519–7526.

(22) Hadda, T. B.; LeBozoc, H. *Polyhedron* **1988**, *7*, 575.

(23) Maerker, G.; Case, F. H. *J. Am. Chem. Soc.* **1958**, *80*, 2745–2748.

(24) Jensen, K. A.; Henriksen, L. *Acta Chim. Scand.* **1968**, *22*, 1107.

(25) Cummings, S. D.; Eisenberg, R. *Inorg. Chem.* **1995**, *34*, 2007–2014.

(26) Bahr, G.; Schleitzer, G. *Chem. Ber.* **1957**, *90*, 438.

(27) Perrin, D. D.; Armarego, W. L. F. *Purification of Laboratory Chemicals*, 3rd ed.; Pergamon Press: Oxford, 1988.

(28) Hodges, K. D.; Rund, J. V. *Inorg. Chem.* **1975**, *14*, 525.

Pt(tmphen)(tdt) (6). A sample of 105.0 mg (0.2090 mmol) of Pt-(tmphen)Cl₂ was placed in a round bottom flask under N₂ and dissolved in 15 mL of hot DMSO. To this was added a solution of 0.05 mL of H₂tdt (0.3772 mmol) and excess KOH in methanol. A bright red solution and precipitate formed immediately and was stirred for an additional 20 min. Excess water was added to the cooled mixture, and the fine red precipitate was filtered, washed repeatedly with water and Et₂O, and dried under vacuum. Yield was 70% based on Pt. Small samples were recrystallized with CH₂Cl₂: ¹H NMR (CD₂Cl₂) δ 9.16 (2 H, s), 8.12 (2 H, s), 7.22 (1 H, d, *J* = 8 Hz), 7.16 (1 H, s), 6.61 (1 H, d, *J* = 8 Hz), 2.62 (6 H, br s), 2.26 (3 H, s). Anal. Calcd for PtC₂₃H₂₂N₂S₂: C, 47.17; H, 3.79. Found C, 46.80; H, 3.69.

Pt(dbbpy)(tdt) (7). A 268.0 mg (0.5015 mmol) sample of Pt-(dbbpy)Cl₂ was placed in a round-bottom flask under N₂ and partially dissolved in a mixture of 30 mL of acetone and 20 mL of dichloromethane. To this was added a solution of 0.08 mL (0.6036 mmol) of K₂tdt and excess KOH in methanol. A bright purple solution formed immediately and was stirred for an additional 2 h. The solvents were removed under vacuum, and the product was redissolved in dichloromethane and filtered. The filtrate was poured into cold hexanes to precipitate the bright purple product, which was then filtered, washed several times with diethyl ether, hexanes and isopropanol/H₂O, and dried under vacuum: 251.5 mg of product were isolated (81% yield based on Pt); ¹H NMR (DMSO-*d*₆) δ 8.94 (2 H, d, *J* = 6.0 Hz), 8.63 (2 H, s), 7.77 (2 H, s), 7.07 (1 H, d, *J* = 8.0 Hz), 7.00 (1 H, s), 6.52 (1 H, d, *J* = 8.0 Hz), 2.17 (3 H, s), 1.42 (18 H, s). Anal. Calcd for PtC₂₅H₃₀N₂S₂: C, 48.61; H, 4.84. Found C, 48.54; H, 4.84.

Pt(dmbpy)(tdt) (8). This complex was prepared using the general method described for Pt(dbbpy)(tdt) using 301.0 mg of Pt(dmbpy)Cl₂ and 0.2 mL of H₂tdt: 406.0 mg of red-purple product was isolated (95% yield based on Pt); ¹H NMR (DMSO-*d*₆) δ 8.87 (2 H, d, *J* = 6.0 Hz), 8.52 (2 H, s), 7.61 (2 H, d, *J* = 6.0 Hz), 7.06 (1 H, d, *J* = 7.6 Hz), 6.99 (1 H, s), 6.51 (1 H, d, *J* = 8.8 Hz), 2.46 (3 H, s), 2.17 (3 H, s), 2.07 (3 H, s). Anal. Calcd for PtC₁₉H₁₈N₂S₂: C, 42.72; H, 3.40. Found C, 42.32; H, 3.36.

Pt(bpy)(tdt) (9). This complex was prepared using the method described for Pt(dbbpy)(tdt) using 195.5 mg of Pt(bpy)Cl₂ and 0.1 mL of H₂tdt: 200.5 mg dark purple product isolated (86% yield based on Pt); ¹H NMR (DMSO-*d*₆) δ 9.08 (2 H, d, *J* = 6.0 Hz), 8.66 (2 H, d, *J* = 8.0 Hz), 8.37 (2 H, dd, *J* = 8 Hz), 7.77 (2 H, m), 7.08 (1 H, d, *J* = 8.0 Hz), 7.01 (1 H, s), 6.53 (1 H, dd, *J* = 1.2 Hz, *J* = 7.6 Hz), 2.18 (3 H, s). Anal. Calcd for PtC₁₇H₁₄N₂S₂: C, 40.39; H, 2.79. Found C, 40.62; H, 2.65.

Pt(phen)(tdt) (10). This complex was prepared using the method described for Pt(dbbpy)(tdt) using 192.0 mg of Pt(phen)Cl₂ and 0.07 mL of H₂tdt: 213.0 mg of dark purple product was isolated (93% yield based on Pt); ¹H NMR (DMSO-*d*₆) δ 9.39 (2 H, d, *J* = 5.1 Hz), 8.89 (2 H, d, *J* = 8.6 Hz), 8.27 (2 H, s), 8.10 (2 H, m), 7.12 (1 H, d, *J* = 8.2 Hz), 7.05 (1 H, s), 6.56 (1 H, d, *J* = 7.4 Hz), 2.20 (3 H, s). Anal. Calcd for PtC₁₉H₁₄N₂S₂: C, 43.10; H, 2.66. Found C, 42.86; H, 2.42.

Pt(Cl-phen)(tdt) (11). This complex was prepared using the method described for Pt(dbbpy)(tdt) using 268.0 mg of Pt(Cl-phen)Cl₂ and 0.08 mL of H₂tdt: 291.5 mg of a bright blue product was isolated (93% yield based on Pt); ¹H NMR (DMSO-*d*₆) δ 9.40 (1 H, m), 9.32 (1 H, m), 9.02 (1 H, m), 8.87 (1 H, d, *J* = 8.4 Hz), 8.54 (1 H, s), 8.16 (1 H, m), 8.07 (1 H, m), 7.08 (1 H, d, *J* = 8.0 Hz), 7.02 (1 H, s), 6.56 (1 H, d, *J* = 8.0 Hz), 2.21 (3 H, s). Anal. Calcd for PtC₁₉H₁₃ClN₂S₂: C, 40.46; H, 2.32. Found C, 40.37; H, 2.45.

Pt(Cl₂bpy)(tdt) (12). This complex was prepared using the method described for Pt(dbbpy)(tdt) using 181.5 mg of Pt(Cl₂bpy)Cl₂ and 0.1 mL of H₂tdt: 112.5 mg of blue-green product was obtained, but column chromatography on alumina was necessary to isolate the desired product from two other unknown products (less than 20% yield based on Pt); ¹H NMR (DMSO-*d*₆) δ 8.95 (2 H, d, *J* = 6.0 Hz), 8.92 (2 H, d, 2.4 Hz), 7.88 (2 H, d, 6.4 Hz), 7.06 (1 H, d, *J* = 7.6 Hz), 6.98 (1 H, s), 6.54 (1 H, d, *J* = 8 Hz), 2.18 (3 H, s).

Pt(EC-bpy)(tdt) (13). This complex was prepared using the method described for Pt(dbbpy)(tdt) using 317.0 mg of Pt(EC-bpy)Cl₂ and 0.1 mL of H₂tdt: 188.5 mg of green product was isolated (58% yield based on Pt); ¹H NMR (DMSO-*d*₆) δ 9.28 (2 H, d, *J* = 6.0 Hz), 9.00 (2 H, s), 8.13 (2 H, br), 7.11 (1 H, d, *J* = 8.0 Hz), 7.03 (1 H, s), 6.57 (1 H, d, *J* = 7.2 Hz), 4.45 (4 H, q, *J* = 7.2 Hz), 2.19 (3 H, s), 1.40 (6 H, t,

J = 7.2 Hz). Anal. Calcd for PtC₂₃H₂₂N₂O₄S₂: C, 42.52; H, 3.41. Found C, 42.49; H, 3.33.

Spectroscopic Characterization. ¹H NMR spectra were recorded on a Bruker AMX-400 spectrometer operating at 400 MHz. Chemical shifts are reported relative to TMS but were measured based on the internal solvent peak (DMSO-*d*₆, δ 2.49). Infrared spectra were recorded on a Mattson Galaxy 6020 FTIR spectrophotometer, and samples were in KBr pellets. Absorption spectra were recorded on a Hitachi U2000 UV-visible spectrophotometer. Steady-state emission measurements were performed on a Spex Fluorolog-2 fluorescence spectrophotometer equipped with a 450 W Xenon lamp and Hamamatsu R929 photomultiplier tube detector. Room-temperature measurements were made using 1 cm × 1 cm quartz fluorescence cells. Low-temperature emission spectra were recorded in butyronitrile solvent glasses formed in 5 mm diameter glass NMR tubes under vacuum and placed in a liquid nitrogen dewar equipped with quartz windows. Emission was collected at 90° from the excitation for both experiments. Solid-state samples were mounted onto microscope slides or mixed with KBr and placed in thin glass tubes, and emission was collected using a front-face geometry. The emission spectra were corrected for detector sensitivity in the region below 12 500 cm⁻¹, and the excitation spectra were corrected for the lamp intensity variation with wavelength using an internal rhodamine B reference quantum counter.

Emission Quantum Yields. Quantum yields of the complexes were determined relative to cresyl violet in EtOH at 298 K (Φ_r = 0.54).³¹ Samples of the complexes were prepared in CH₂Cl₂, degassed by 4 freeze-pump-thaw cycles in a glass bulb fitted onto a 1 cm × 1 cm Spectrosil quartz cell, and then were placed under an atmosphere of N₂ to prevent leakage of air into the cell. The absorbance of both the sample and the standard at the excitation wavelength were approximately 0.1–0.2. The quantum yields were calculated using eq 1,³² where

$$\Phi_s = \frac{(1 - 10^{-A_s}) \eta_s^2 I_s}{(1 - 10^{-A_r}) \eta_r^2 I_r} \quad (1)$$

A = absorbance of the sample (s) or reference (r) at the excitation wavelength, *l* = 1 cm, *η* = refractive index of the sample or reference solvents, and *I* = integrated emission intensity of the sample or reference.

Emission Lifetimes. Emission lifetimes were determined through time-correlated single-photon counting using excitation wavelengths of 590 or 380 nm. The excitation source was a Quantronix 4000 series Q-switched Nd-YLF laser operating at 37.8 MHz to produce 10 ps pulses. The 1.053 μm fundamental was frequency doubled using a KTP crystal, and the resulting 0.5265 μm light was used to pump a Coherent 700 cavity-dumped dye laser producing 590 nm excitation. Mixing of the 1.053 μm fundamental with the dye output gave the 380 nm excitation. The excitation wavelength was focused into the center of a 1 cm × 1 cm quartz sample cell. The emission was collected at a 90° angle and focused to a monochromator which selected the wavelength of the emission maximum, and the resulting emission was detected by a thermoelectrically-cooled Hamamatsu R3809U-01 photomultiplier tube. The instrument response function at the excitation wavelength was deconvoluted from the luminescence decay, and the decay was fitted using a least-squares method to exponential functions. In addition to a long decay component (0.1–1 μs) of interest, several of the samples displayed a short (<100 ps) decay component. The data were not able to be fit to a biexponential function due to the small number of channels in the region of the fast component, so single exponential fits were used.

Electrochemical Measurements. Cyclic voltammograms were measured using a BAS 100W electrochemical workstation. The electrochemical cell consisted of a glassy-carbon working electrode, a Ag/AgCl reference electrode, and a Pt wire auxiliary electrode in a single compartment. (TBA)PF₆ (0.1 M) in degassed DMF was used

(31) Magde, D.; Brannon, J. H.; Cremers, T. L.; Olmsted, I. J. *J. Phys. Chem.* **1979**, *83*, 696–699.

(32) Demas, N. J.; Crosby, G. A. *J. Am. Chem. Soc.* **1970**, *92*, 7262.

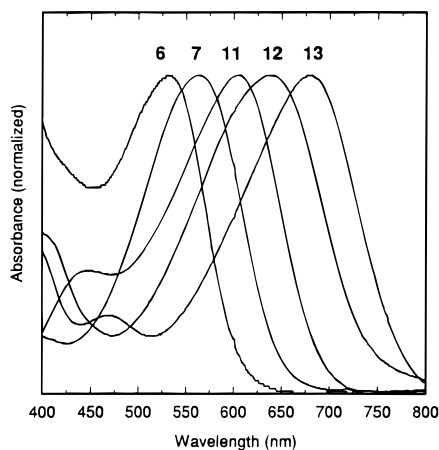


Figure 1. Charge-transfer-to-diimine absorption band for Pt(tmphen)(tdt) (6), Pt(dbppy)(tdt) (7), Pt(Cl-phen)(tdt) (11), Pt(Cl₂bpy)(tdt) (12) and Pt(EC-bpy)(tdt) (13) in dichloromethane. Absorbance maxima have been normalized.

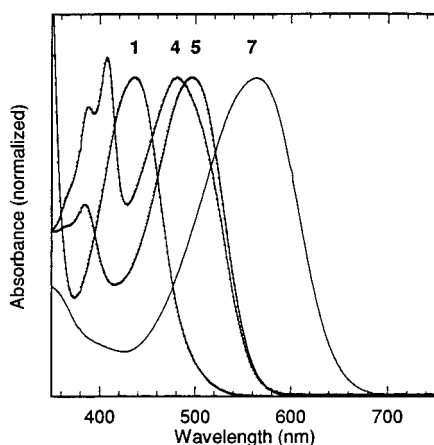


Figure 2. Charge-transfer-to-diimine absorption band for Pt(dbppy)(tbca) (1), Pt(dbppy)(dmqdt) (4), Pt(dbppy)(mnt) (5) and Pt(dbppy)(tdt) (7) in dichloromethane. Absorbance maxima have been normalized.

as the electrolyte, and an internal ferrocene/ferrocenium couple (0.40 V vs NHE) was used to calibrate the cell potential.³³

Results

Syntheses. The complexes in this study were synthesized following established methods, characterized by ¹H NMR and infrared and UV–visible spectroscopies, and found to be analytically pure by elemental analyses. All of the compounds are air stable as solids, even at temperatures up to 150–200 °C. The complexes with tdt or edt as the dithiolate are sensitive to air and light when in solution, so all samples used for spectroscopic study were freshly prepared. The other dithiolate complexes are stable in ambient solution for several days.

Absorption Spectra. The absorption spectra of all of the complexes were measured, and the pertinent results are summarized in Table 1. The absorption maxima are listed for only the lowest-energy band in dichloromethane, although each complex possesses additional absorption features at higher energies. The absorption spectra for several of the complexes are presented in Figures 1 and 2. Molar absorptivities in dichloromethane were obtained for complexes with sufficient solubility, and values range from ~7000–13 000 M⁻¹ cm⁻¹.

The positions of the lowest-energy absorption maxima for all of the complexes are dependent on the solvent. Because

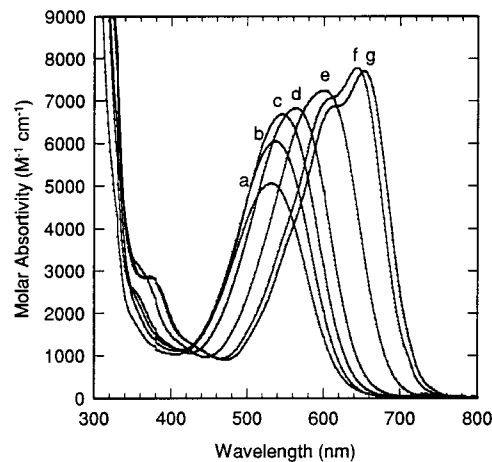


Figure 3. Charge-transfer-to-diimine absorption band for Pt(dbppy)(tdt) in (a) CH₃CN, (b) DMSO, (c) DMF, (d) THF, (e) CH₂Cl₂, (f) benzene and (g) toluene.

the solvatochromic shifts yield information regarding the nature of the excited state, solvatochromic measurements were conducted for each complex. The CT absorption band for Pt(dbppy)(tdt) is shown in Figure 3 for six solvents of differing polarity. The high solubility of this complex in a variety of organic solvents allowed for a detailed investigation of its solvatochromic behavior. Absorption spectra were obtained in 13 solvents, and the solvent-induced shifts in energy were measured. Solvatochromic measurements for each of the other complexes were made using a minimum of 10 solvents. Plots of the energies of the CT band maxima vs solvent polarity parameters gave excellent linear correlations using Kosower's Z and Lees' E*_{MLCT} solvent scales except for some deviations with dichloromethane and chloroform. Other solvent scales such as Kamlet's π* scale, Dong's Py scale, Hildebrand's δ scale, and Gutmann's AN and DN solvent parameters gave considerably weaker correlations. Since all of the complexes exhibited similar solvatochromic properties and since relative trends in solvent-dependent CT energies were important in the present study, an empirical solvent scale based on the results for Pt(dbppy)(tdt) was devised to determine the relative degree of solvatochromism of the other complexes.³⁴ The data for complexes 1–13 fit well (r² > 90%) to this scale, and the slopes of those plots, which are listed in Table 1, are all of similar magnitude. Increases in the solvent polarity also have the effect of decreasing the molar extinction coefficient of the CT transition. For example, the molar extinction coefficient at the maximum of the Pt(dbppy)(tdt) absorption band is 8100 M⁻¹ cm⁻¹ in toluene, 7200 M⁻¹ cm⁻¹ in CH₂Cl₂, and 6500 in DMSO. The integrated area of this CT band decreases by over 20% in going from toluene to DMSO.

Emission Spectra. Photoluminescence has been detected for all of the complexes in the solid state, fluid solution, and frozen solvent glasses. The emission spectra for several compounds in butyronitrile glass at 77 K are presented in Figures 4 and 5. The energy maxima for fluid solution and frozen glass solution samples of each complex are included in Table 1. The 77 K emission maxima range from 496 to 784 nm, a shift of over 7400 cm⁻¹ with variation in the diimine and dithiolate ligands. For most of the tdt complexes, the 77 K emission profiles are asymmetric with shoulders separated from the emission maxima by approximately 1250–1300 cm⁻¹. For the series of dbppy

(33) Gagné, R. R.; Koval, C. A.; Lisensky, G. C. *Inorg. Chem.* **1980**, *19*, 2854–2855.

(34) Pt(NN)(SS) solvent parameters: CCl₄(0.000), toluene (0.172), benzene (0.218), THF (0.494), chloroform (0.610), 3-pentanone (0.676), pyridine (0.743), 1,2-dichloroethane (0.758), dichloromethane (0.765), acetone (0.797), DMF (0.901), DMSO (0.973), acetonitrile (1.000).

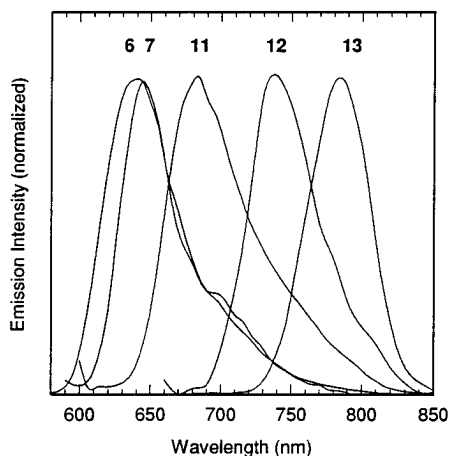


Figure 4. Charge-transfer-to-diimine emission band for Pt(tmphen)(tdt) (6), Pt(dbppy)(tdt) (7), Pt(Cl-phen)(tdt) (11), Pt(Cl₂bpy)(tdt) (12) and Pt(EC-bpy)(tdt) (13) in frozen butyronitrile at 77 K. Emission intensities have been normalized.

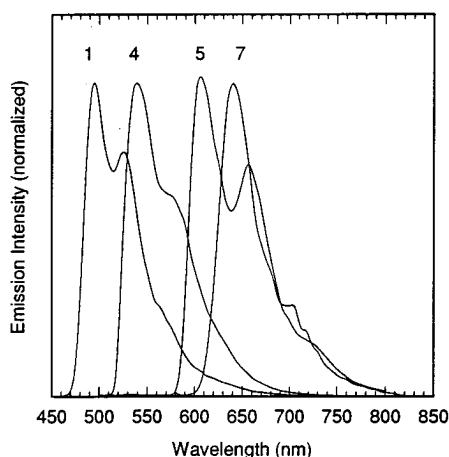


Figure 5. Charge-transfer-to-diimine emission band for Pt(dbppy)(tbcda) (1), Pt(dbppy)(dmqdt) (4), Pt(dbppy)(mnt) (5) and Pt(dbppy)(tdt) (7) in frozen butyronitrile at 77 K. Emission intensities have been normalized.

Table 1. CT Absorption and Emission Band Maxima, Molar Extinction Coefficients, and Solvatochromic Shifts of Pt(diimine)(dithiolate) Complexes 1–13^e

compd	absorption λ_{\max} CH ₂ Cl ₂ , 298 K ^a	solvato- chromic shift ^b	emission λ_{\max} CH ₂ Cl ₂ , 298 K ^c	emission λ_{\max} BuCN, 77 K ^d
Pt(dbppy)(tbcda) (1)	437 (12,900)	0.43	590	496
Pt(dbppy)(cpdt) (2)	434 (10,500)	0.33	597	496
Pt(dbppy)(edt) (3)	480 (5900)	0.38	615	628
Pt(dbppy)(dmqdt) (4)	481 (6800)	0.38	618	539
Pt(dbppy)(mnt) (5)	497 (5800)	0.32	620	607
Pt(tmphen)(tdt) (6)	532 (7160)	0.38	675	638
Pt(dbppy)(tdt) (7)	563 (7200)	0.41	720	641
Pt(dmbpy)(tdt) (8)	564	0.41	720	662
Pt(bpy)(tdt) (9)	586 (7350)	0.41	735	666
Pt(phen)(tdt) (10)	583	0.39	730	674
Pt(Cl-phen)(tdt) (11)	605 (7110)	0.36	760	683
Pt(Cl ₂ -bpy)(tdt) (12)	630	0.26	775	739
Pt(EC-bpy)(tdt) (13)	679 (10,400)	0.33	795	784

^a ± 1 nm (molar extinction coefficient in M⁻¹ cm⁻¹). ^b Unitless slope from plot of E_{abs} vs Pt(NN)(SS) empirical solvent parameter. ^c ± 10 nm. ^d ± 2 nm. ^e All maxima in nm.

complexes 1–5 and 7, the structure of the 77 K emission is more pronounced for most of the complexes, with well-defined features having a 1220–1230 cm⁻¹ energy separation (Figure 5).

Table 2. Photoluminescent Properties of Pt(diimine)(dithiolate) Complexes 1–13 in Dichloromethane at 298 K

compd	E_{em} (eV) ^a	Φ_{em}^b	τ (ns) ^c	τ_0 (μ s)	k_r (μ s ⁻¹)	k_{nr} (μ s ⁻¹)
Pt(dbppy)(tbcda) (1)	2.51	12	2.0	1.6	0.62	499
Pt(dbppy)(cpdt) (2)	2.50	2.2	1.5	0.6	0.15	690
Pt(dbppy)(edt) (3)	1.97	2.8	10	32	0.028	111
Pt(dbppy)(dmqdt) (4)	2.30	64	80	12.4	0.081	12.4
Pt(dbppy)(mnt) (5)	2.04	1.0	3	29	0.035	333
Pt(tmphen)(tdt) (6)	1.94	57.0	1020	178	0.0056	0.98
Pt(dbppy)(tdt) (7)	1.93	10.8	504	465	0.0022	2.0
Pt(dmbpy)(tdt) (8)	1.87	7.4	381	517	0.0019	2.6
Pt(bpy)(tdt) (9)	1.86	3.1	291	933	0.0011	3.4
Pt(phen)(tdt) (10)	1.84	6.7	517	773	0.0013	1.9
Pt(Cl-phen)(tdt) (11)	1.81	2.6	315	1207	0.00083	3.2
Pt(Cl ₂ -bpy)(tdt) (12)	1.68	0.43	157	3639	0.00027	6.4
Pt(EC-bpy)(tdt) (13)	1.58	0.04	68	18970	0.000053	15

^a From emission maxima in butyronitrile at 77 K. ^b $\times 10^{-4}$. ^c $\pm 10\%$.

Table 3. Ground- and Excited-State Redox Properties of Pt(diimine)(dithiolate) Complexes 1–13^f

compd	E_{em} (eV)	$E(\text{Pt}^{0/-})^a$	$E(\text{Pt}^{+/0})^b$	$E(\text{Pt}^{*/-})^c$	$E(\text{Pt}^{*/+})^d$
Pt(dbppy)(tbcda) (1)	2.51	-1.302	0.963	1.21	-1.55
Pt(dbppy)(cpdt) (2)	2.50	-1.274	0.957	1.23	-1.54
Pt(dbppy)(edt) (3)	1.97	-1.484	0.431	0.49	-1.54
Pt(dbppy)(dmqdt) (4)	2.30	-1.334	0.814	0.97	-1.49
Pt(dbppy)(mnt) (5)	2.04	-1.266	0.944	0.77	-1.10
Pt(tmphen)(tdt) (6)	1.94	-1.495	0.347	0.45	-1.60
Pt(dbppy)(tdt) (7)	1.93	-1.398	0.389	0.54	-1.55
Pt(dmbpy)(tdt) (8)	1.87	-1.371	0.390	0.50	-1.48
Pt(bpy)(tdt) (9)	1.86	-1.339	0.376 ^c	0.52	-1.49
Pt(phen)(tdt) (10)	1.84	-1.319	0.376 ^c	0.52	-1.46
Pt(Cl-phen)(tdt) (11)	1.81	-1.257	0.359 ^c	0.56	-1.46
Pt(Cl ₂ -bpy)(tdt) (12)	1.68	-1.043	0.380	0.64	-1.30
Pt(EC-bpy)(tdt) (13)	1.58	-0.962	0.412	0.62	-1.17

^a $E_{1/2}$ from reversible couple. ^b E_p anodic peak potential from irreversible couple. ^c Quasi-reversible couple. ^d Calculated from eq 4a. ^e Calculated from eq 4b. ^f All potentials in volts vs NHE unless otherwise noted.

Quantum yields of emission, as determined relative to cresyl violet, and emission lifetimes were measured for each complex in dichloromethane at 298 K, and the results are given in Table 2. From these results, the radiative and nonradiative decay rate constants were calculated according to eqs 2 and 3

$$k_r = \Phi/\tau \quad (2)$$

$$k_{\text{nr}} = 1/\tau - k_r \quad (3)$$

where the temperature dependence of the lifetimes has not been considered. The quantum yield for Pt(dbppy)(tdt) was determined at 15 different excitation wavelengths in the region of the absorption band (440–650 nm). No increase in quantum yield was found in the low-energy region of this band.

Electrochemistry. Cyclic voltammetry was used to determine ground-state redox potentials for complexes 1–13. The potentials and reversible nature of each redox process are listed in Table 3. In general, the complexes each display two reduction waves within the solvent window. The first is reversible for each, and the second is reversible for most of the complexes but only quasi-reversible for the others. The oxidation waves are generally chemically irreversible, although three of the complexes (9–11) display quasi-reversible waves. The anodic and cathodic peak separation and i_p^c/i_p^a current ratio indicate that each reversible redox process corresponds to a single electron transfer.

Excited-state redox potentials have been calculated based on a simple thermodynamic cycle and the observed electrochemical

Table 4. Bimolecular Electron Transfer Rate Constants for Pt(dbbpy)(dithiolate) Complexes **2**, **4**, **5**, and **7** with Aromatic Amine Donors^a

	DMA	TMB	TMPD
Pt(dbbpy)(tbcda) (2)	4×10^9	9×10^9	2×10^{10}
Pt(dbbpy)(dmqdt) (4)	6×10^7	7×10^9	1.2×10^{10}
Pt(dbbpy)(mnt) (5)	$< 10^7$	4×10^8	9×10^9
Pt(dbbpy)(tdt) (7)	4×10^6	3×10^7	5×10^9

^a All values in units of $M^{-1} s^{-1} \pm 15\%$.

results using eq 4

$$E(\text{Pt}^{*/-}) = E(\text{Pt}^{0/-}) + E_{00} \quad (4a)$$

$$E(\text{Pt}^{+/*}) = E(\text{Pt}^{+/0}) - E_{00} \quad (4b)$$

In these calculations, $E_{1/2}$ values from the reversible ground state reductions were used for $E(\text{Pt}^{0/-})$. Because the oxidation steps were irreversible, anodic peak potentials were used for the values of $E(\text{Pt}^{+/0})$. The use of these irreversible peak potentials introduces a significant error in the values for $E(\text{Pt}^{+/*})$. However, as will be discussed below, the oxidation potentials of the tdt complexes of interest (**6**, **7**, **10**, and **11**) change very little due to the common HOMO that they possess. The E_{00} transitions have been estimated using the energy maxima of the 77 K emission in butyronitrile given in Table 1. The use of eqs 4a and 4b ignores differences between E_{00} and the emission maxima, E_{em} , as well as any effects arising from differences in the solvent used for the electrochemical experiments relative to that used in the spectroscopic experiments. Only the relative trends in the calculated excited-state redox potentials are of interest for this study.

Quenching Experiments. Electron-transfer quenching of the excited states of several complexes were explored using both nitroaromatic electron acceptors and aromatic amine electron donors. Reductive quenching experiments were conducted using the Pt(dbbpy)(dithiolate) complexes **1**, **4**, **5**, and **7** in combination with *N,N*-dimethylaniline, *N,N,N,N*-tetramethylbenzidine, and *N,N,N,N*-tetramethyl-1,4-phenylenediamine. A series of at least four samples of each complex were prepared under a nitrogen atmosphere at $\sim 10^{-5}$ M concentrations in CH_2Cl_2 , having amine concentrations, $[Q]$, ranging from 0 – 10^{-2} M. The observed decreases in emission intensity, I_0/I , with increasing amine concentration were analyzed using the Stern–Volmer expression for bimolecular quenching

$$I_0/I = 1 + K_{SV}[Q] \quad (5)$$

Bimolecular electron-transfer rate constants, k_{el} , were calculated from the lifetimes in the absence of quencher, τ_0 , and the Stern–Volmer constants K_{SV} using the relation of eq 6

$$k_{el} = K_{SV}/\tau_0 \quad (6)$$

The results of these experiments are presented in Table 4. Electron-transfer rates range from below $4 \times 10^{-6} s^{-1}$ up to the diffusional limit, depending on the choice of complex and amine quencher.

Oxidative quenching experiments were conducted with the Pt(diimine)(tdt) complexes **6**, **7**, **10**, and **11** in combination with nitrobenzene, *p*-nitrobenzaldehyde, and *p*-dinitrobenzene using the same methodology as described above. The results are presented in Table 5. The range of electron-transfer rates obtained from the oxidative quenching experiments appears to be somewhat less than that measured for the reductive quenching

Table 5. Bimolecular Electron Transfer Rate Constants for Pt(diimine)(tdt) Complexes **6**, **7**, **10**, and **11** with Nitroaromatic Acceptors^a

	nitrobenzene	nitrobenzaldehyde	dinitrobenzene
Pt(tmphen)(tdt) (2)	7.9×10^9	1.5×10^{10}	2.3×10^{10}
Pt(dbbpy)(tdt) (4)	9.5×10^8	7.6×10^9	1.2×10^{10}
Pt(bpy)(tdt) (5)	8.0×10^8	6.3×10^9	1.1×10^{10}
Pt(Cl-phen)(tdt) (7)	5×10^7	1.0×10^9	8.2×10^9

^a All values in units of $M^{-1} s^{-1} \pm 15\%$.

experiments and will be discussed below in regard to the excited-state redox potentials of the complexes.

Discussion

The complexes **1**–**13** have been prepared in order to study the electronic effects that diimine and dithiolate ligands have on the charge-transfer and photoluminescent properties of the Pt(diimine)(dithiolate) chromophore. For the purposes of discussion, the complexes can be divided into two groups. Complexes **6**–**13** are Pt(diimine)(tdt) complexes that differ only in the functional groups on the 2,2'-bipyridine or 1,10-phenanthroline chelating ligands, and complexes **1**–**5** and **7** are Pt-(4,4'-di-*tert*-butyl-2,2'-bipyridine)(dithiolate) complexes that differ only in the dithiolate.

The complex Pt(bpy)(tdt) was originally prepared and reported by Vogler and Kunkely who observed the solvatochromic absorption band as well as emission in frozen EtOH glass at 77 K.³⁵ Both transitions were assigned as LLCT, based on the previous work of Miller and Dance,³⁶ and no emission was detected in solution at room temperature. Pt(bpy)(tdt) and Pt(phen)(tdt) were later studied by Srivastava in the context of $^1\text{O}_2$ generation by the excited states of the complexes, but no photoluminescence was reported.³⁷

Nature of the Excited States. In early work with square-planar Ni(II), Pd(II), and Pt(II) complexes having dithiolate donor ligands and diimine acceptor ligands, the low-energy solvatochromic absorption bands were assigned to ligand-to-ligand charge-transfer (LLCT) transitions, involving a HOMO localized on the dithiolate, a LUMO localized on the diimine, and little or no metal orbital involvement. More recent work from our laboratory indicates that the HOMO in these complexes contains a significant contribution from metal orbitals in addition to dithiolate-based functions.²⁰ This conclusion was based on comparison of the absorption spectra of M(diimine)(dithiolate) complexes with M = Ni(II), Pd(II), and Pt(II) as well as molecular orbital calculations on related complexes. Since the excited state is not purely LLCT or MLCT in character, we have adopted the more general term charge-transfer-to-diimine, and a full discussion of this assignment has been presented recently.²⁵ In order to analyze the tuning of the Pt(diimine)(dithiolate) excited states, it is important to establish first that the excited state corresponding to the solvent-dependent absorption band has the same orbital nature for all of the complexes. Other excited states of different orbital character may lie close in energy, including charge-transfer-to-dithiolate, intraligand, and metal-centered states.

The absorption bands of all of the complexes possess the same basic features. Intense ($\epsilon \geq 20\,000 M^{-1} \text{cm}^{-1}$) absorptions are found in the near UV region of the spectrum that do not shift in energy with changes in solvent. The energies are very close to those of uncoordinated diimine and dithiolate ligands,

(35) Vogler, A.; Kunkely, H. *J. Am. Chem. Soc.* **1981**, *103*, 1559.(36) Miller, T. R.; Dance, G. *J. Am. Chem. Soc.* **1973**, *95*, 6790.(37) Shukla, S.; Kamath, S. S.; Srivastava, T. S. *J. Photochem. Photobiol., A: Chem.* **1989**, *50*, 199–207.

and therefore the bands are assigned to intraligand (IL) $\pi-\pi^*$ transitions. No further consideration to these IL states will be given.

The charge-transfer-to-diimine transition appears for each complex as an intense ($\epsilon \cong 5000-13\,000\text{ M}^{-1}\text{ cm}^{-1}$) band in the visible region of the spectrum at energies where the uncoordinated ligands do not absorb. The complexes display characteristic solvatochromic effects due to the dipolar charge distribution in the ground state and a charge-transfer axis that lies colinear with the dipole axis. The observed shift of band maxima to higher energy in solvents of increasing polarity is indicative of a polar ground state and nonpolar excited state. This is in contrast to the small degree of solvatochromism observed for the MLCT bands of transition metal diimine complexes such as $\text{Ru}(\text{bpy})_3^{2+}$ and related systems. For those cases, the MLCT band maxima shift to lower energy with increasing solvent polarity, indicative of a nonpolar ground state and more polar excited state.³⁸ Similar small solvatochromic shifts are observed for the charge-transfer-to-dithiolate absorption bands of transition metal dithiolate complexes that do not contain diimine ligands.³⁹ The charge-transfer-to-diimine assignment is supported by the fact that all of the complexes presented here have large negative solvatochromic shifts of similar magnitude (Table 1).

Photoluminescence is observed for all of the complexes in this study in the solid state, frozen solvent glass and, most importantly, fluid solution media. The last observation is in contrast to previous work by Vogler and Kunkely, who reported that no detectable emission was observed from solution samples of $\text{Pt}(\text{bpy})(\text{tdt})$.³⁵ Complexes of $\text{Pt}(\text{II})$ having diimine and/or dithiolate ligands have been investigated for which photoluminescence has been assigned to originate from excited states that are diimine intraligand, metal-to-diimine charge-transfer, metal centered, and metal-to-dithiolate charge-transfer in nature as well as from excited states that are mixtures of these contributions. In more concentrated solutions of $\text{Pt}(\text{II})$ diimine complexes ($10^{-3}-10^{-4}\text{ M}$), excimer emission has also been observed. In previous studies from our laboratory on solution-luminescent $\text{Pt}(\text{diimine})(\text{dithiolate})$ complexes, emission has been assigned to involve charge-transfer-to-diimine states except for some mnt complexes in which case the charge-transfer-to-dithiolate assignment has been proposed. The orbital nature and spin character of the emissive states for complexes **1-13** can be elucidated on the basis of the emission energies, structure, quantum yields, and lifetimes as well as on electrochemical redox potentials.

The emission spectra observed for the complexes **1-13** are broad ($\sim 20\,000\text{ cm}^{-1}$ FWHM) and featureless in dilute room temperature solutions ($10^{-5}-10^{-6}\text{ M}$). The intensities, band-shapes, and energies of the emission spectra for complexes **1-13** are characteristic of emission from CT states.⁴⁰ The quantum yields of emission, which are in the range of $10^{-3}-10^{-4}$ for most of the complexes, rule out metal-centered emissive states, from which observable solution luminescence is unknown for $\text{Pt}(\text{II})$ chromophores. Emission in fluid solution from diimine intraligand (IL) excited states is rare, although not unknown.¹⁷ The highest emission energies from complexes **1-13** are significantly lower than is typical for luminescence from uncoordinated diimines, which argues against assignment of an IL emitting state. The high degree of structure typically associated with diimine IL emission is not found for complexes

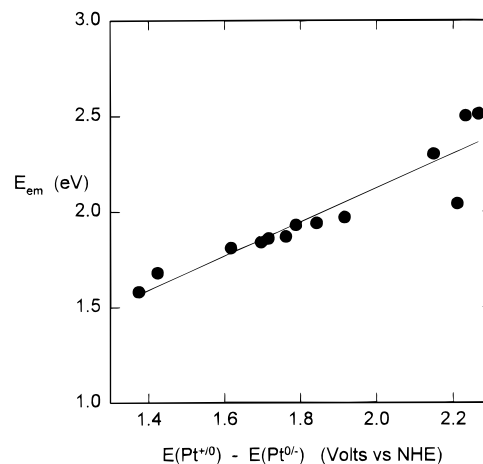


Figure 6. Plot of E_{em} (77 K, butyronitrile) vs. the difference between the ground state oxidation and reduction potentials for complexes **1-13** and linear least-squares fit to the data.

1-13, the broad emission profiles of which are typical of charge-transfer luminescence.

The energies of the emission maximum depend on both the diimine and dithiolate, as presented in Table 1, although the emission band maxima are somewhat approximate because of the broad nature of the emission profile in fluid solution. In frozen butyronitrile solutions at 77 K, the emission profiles shift to higher energy and sharpen ($\sim 12\,000\text{ cm}^{-1}$ FWHM), displaying an increased degree of structure and well-defined emission maxima. The blue-shift for all of the complexes in going from fluid solution to frozen solvent glass is a common rigidochromic effect observed for many metal diimine complexes.⁴¹ The 77 K emission data reveal that the emission energy changes with the diimine and dithiolate ligands in the same way as that described above for the absorption band maxima. A plot of the emission energy vs the absorption energy for complexes **1-13** gives a strong correlation, indicating that the orbital nature of the absorbing and emitting states are the same.

Additional support for the orbital nature of the excited state comes from the electrochemical data. The formation of a charge-transfer-to-diimine excited state formally involves the oxidation of a HOMO having dithiolate and metal orbital character and reduction of a diimine-based LUMO. A linear correlation should exist between the energy of the CT excited state and the difference between the ground state oxidation and reduction potentials. This correlation has been observed for numerous transition metal diimine complexes, although none has been reported for a $\text{Pt}(\text{II})$ complex.⁴¹⁻⁴⁴ The ground state redox potentials listed in Table 3 display the general trend that electronic effects of the diimine influence the reduction potentials, whereas the nature of the dithiolate influences the oxidation potentials. Presented in Figure 6 is a plot of the difference in electrochemical potentials against the emission energies for complexes **1-13**. A good correlation exists between the difference in the ground state redox potentials and the emission energies. A linear correlation also exists when using the absorption energies, in accord with the aforementioned correlation between absorption and emission energies. These observations strongly support the notion that the complexes share a common charge-transfer-to-diimine excited state.

While excimer emission has been observed for a number of

(38) Ford, W. E.; Calvin, M. *Chem. Phys. Lett.* **1980**, *76*, 105-108.

(39) Bevilacqua, J. M.; Zuleta, J. A.; Eisenberg, R. *Inorg. Chem.* **1994**, *32*, 3689.

(40) Kalyanasundaram, K. *Photochemistry of Polypyridine and Porphyrin Complexes*; Academic Press: New York, 1992.

(41) Juris, A.; Balzani, V.; Barigelletti, F.; Campagna, S.; Belser, P.; Von Zelewsky, A. *Coord. Chem. Rev.* **1988**, *84*, 85-277.

(42) Rillema, D. P. *Inorg. Chem.* **1983**, *22*, 1617.

(43) Caspar, J. V.; Meyer, T. J. *Inorg. Chem.* **1983**, *22*, 2444-2453.

(44) Rezvani, A. R.; Crutchley, R. J. *Inorg. Chem.* **1994**, *33*, 170-174.

related Pt(II) chromophores,^{16,45,46} there is no evidence for excimer emission in the 298 K solutions of the complexes studied here. For all of the emission measurements of **1–13**, the solution concentrations were on the order of 10^{-5} M, which is too dilute for excimers to form to an observable extent. The reports of excimers involving other Pt(II) complexes were obtained from solutions having concentrations in the 10^{-3} – 10^{-4} M range.^{16,45,46} Recently, Crosby has reported excimer emission from Pt(dpphen)(ecda) and Pt(dmbpy)(ecda) at 77 K in concentrated solvent glasses.⁴⁷ In the present study, the 77 K emission spectra were obtained from dilute solutions that upon warming exhibited red-shifts to give the observed room temperature emission bands. The energy shifts agree with previous observations of rigidochromic shifts in emission energy^{48–50} and contrast with that suggested by Crosby.⁴⁷

The spin character of the emissive state is assigned to be different from that of the ground state, making the photoluminescence a formally spin-forbidden process, although the purity of the spin states and selection rules is substantially reduced in heavy-metal complexes such as those of Pt(II). Intrinsic lifetimes in the microsecond range and separations between the lowest-energy absorption and highest-energy emission bands for complexes **1–13** are indicative of metal complex phosphorescence. The efficiency of intersystem crossing to the triplet state, Φ_{isc} , is often assumed to be unity for second- and third-row transition metal chromophores, based on the early work with Ru(bpy)₂²⁺ and Os(bpy)₂²⁺ by Demas and Crosby.³² They proposed that, if Φ_{isc} is less than unity, excitation into a region where the spin-forbidden singlet-triplet absorption is expected to lie will give rise to a quantum yield larger than that found when excitation occurs at regions of primarily spin-allowed absorption. Although there is no feature in the absorption spectrum of Pt(dbbpy)(tdt) which can be directly attributed to a singlet-triplet CT transition, bands of this type typically are either buried underneath the more intense singlet-singlet CT band or appear as low-energy shoulders. Excitation in the low-energy region of the absorption spectrum does not lead to an increase in the emission quantum yield for Pt(dbbpy)(tdt). We interpret this result to indicate that the complexes in this study, like other second- and third-row transition metal diimine complexes, have an intersystem crossing efficiency of near unity.

Tuning the Excited-State Energy. The orbital nature of the charge-transfer-to-diimine excited state has been discussed in terms of contributions from both the dithiolate and the diimine ligands. This orbital picture predicts that variation in the electronic properties of the diimine and dithiolate ligands should have an effect on the excited-state energy. An important goal of this study has been to investigate the range of energy tuning which can be accomplished through ligand variation and to determine if the changes in energy support the charge-transfer-to-diimine assignment.

The dependence of the CT absorption band energies on the diimine has been probed using the Pt(diimine)(tdt) complexes **6–13**. Changes in the nature of substituents on the bpy or phen backbone of this chromophore affect the energy of the LUMO, which is localized on the diimine. Substituents on the diimine have a much smaller or even negligible effect on the HOMO, although changes in diimine basicity may have a modest influence on the energy of the metal orbitals involved in the

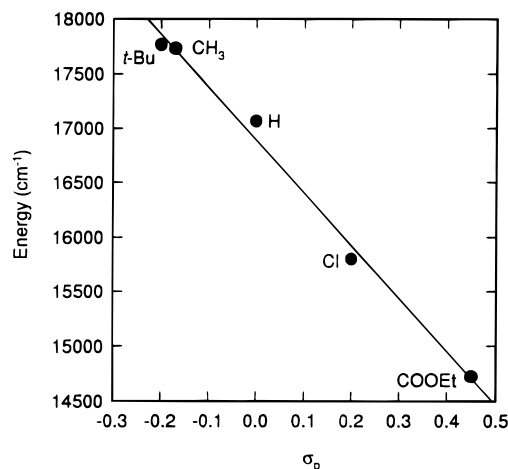


Figure 7. Plot of E_{em} (77 K, butyronitrile) vs. the Hammett constant for Pt(4,4'-X-2,2'-bpy)(tdt) complexes **7**, **8**, **9**, **12**, and **13** with a linear least-squares fit to the data.

HOMO. Those diimines which possess electron-donating alkyl substituents have the effect of raising the energy of the LUMO and the consequent energy gap, while diimines which possess electron-withdrawing substituents such as chloro and ethylcarboxy groups have the effect of lowering the energy of the LUMO and the energy gap. These shifts agree well with the inductive influence of the substituent. For example, a plot of the CT absorption energy vs the Hammett substituent constant of the complexes with 4,4'-X-2,2'-bipyridine ligands (X = t-Bu, Me, H, Cl, COOEt) gives an excellent correlation, as shown in Figure 7. The overall tuning of the CT energy is quite large, especially when compared with other transition metal complexes containing similar bipyridine and phenanthroline derivatives.⁴⁰

The shift in the CT band energy with variation of the dithiolate is also large, spanning over 5100 cm^{-1} , but the effects are not as easy to predict as with the substituent effect of the diimines. The nature of the dithiolate influences the energy of the HOMO, which has substantial dithiolate orbital character, but has almost no effect on the diimine-localized LUMO. The CT absorption band energies increase along the series $tdt < mnt < dmqt \sim edt < tbcda \sim cpdt$. Some empirical observations concerning the electronic structure of the complexes in this series may be noted. First, the CT energies of complexes having 1,1-dithiolates are larger than those of complexes having 1,2-dithiolates, consistent with HOMOs which are lower in energy. This effect is also observed for the charge-transfer-to-dithiolate transitions of homoleptic transition metal bis(dithiolate) complexes.⁵¹ The size of the chelate ring appears to have an important influence on the energy of the HOMO. Second, the transitions for complexes having 1,1-dithiolates have oscillator strengths that are approximately twice as large as those of complexes having 1,2-dithiolates, as seen from the data for molar absorptivity given in Table 1.

The shift of the emission band to lower energies with increasing acceptor strength of the diimine provides strong evidence to support the assignment of a charge-transfer-to-diimine emitting state for all of the complexes. In contrast, complexes having a charge-transfer-to-dithiolate emissive state would not display such a trend because the diimine π^* orbitals are not involved in such a transition. The inductive effect that the substituents on the diimine may have on the energy of the metal orbitals, and hence the energy of a charge-transfer-to-dithiolate excited state, should be smaller and shift the energies

(45) Kunkely, H.; Vogler, A. *J. Am. Chem. Soc.* **1990**, *112*, 5625–5627.

(46) Wan, K.-T.; Che, C.-M.; Cho, K.-C. *J. Chem. Soc., Dalton Trans.* **1991**, 1077–1080.

(47) Kendrick, K. R.; Crosby, G. A., personal communication.

(48) Wrighton, M. *Chem. Rev.* **1974**, *74*, 401–429.

(49) Giordano, P. J.; Bock, C. R.; Wrighton, M. S. *J. Am. Chem. Soc.* **1978**, *100*, 6960–6965.

(50) Zulu, M. M.; Lees, A. *J. Inorg. Chem.* **1989**, *28*, 85–89.

(51) Cummings, S. D.; Eisenberg, R. *Inorg. Chim. Acta*, Submitted for publication.

in the opposite direction. In fact, just such an effect has been observed for square-planar mixed-ligand Pt(II) dithiolate complexes containing phosphine or phosphite ligands, for which the charge-transfer-to-dithiolate (or MLCT) emissive state energies depend on the donicity of the phosphine/phosphite ligands.³⁹ Phosphines which are stronger electron-donors raise the metal orbital energies and lower the charge-transfer-to-dithiolate emission energies, while phosphites which are weaker donors have the reverse effect. The observed shifts are less than 1000 cm^{-1} for these inductive effects.

The influence of the dithiolate on the emission energy is also quite large, with the maximum for Pt(dbbpy)(tdt) (**7**) being 4560 cm^{-1} lower in energy than that for Pt(dbbpy)(tbcda) (**1**). The trend for the series of complexes **1–5**, **7** is very close to that observed in the CT absorption band energies, with the only differences being in the relative ordering of complexes whose energies are very close to each other. The retention of this general trend among the series of Pt(dbbpy)(dithiolate) complexes indicates that all of the complexes share an emitting state of orbital character common to that of the charge-transfer-to-diimine absorbing state.

The results of this study demonstrate that the excited-state energies of the Pt(diimine)(dithiolate) chromophore can be systematically tuned by altering the diimine and dithiolate ligands. The ability to control the absorption and emission energies is important for the development of this chromophore for photocatalytic applications.⁵² The excited-state energy can also play a potentially important role in tuning kinetic and thermodynamic properties of the excited-state complex.

Tuning the Kinetics of Excited-State Decay. In addition to the effects on the emission energy, the diimines and dithiolates also influence the emission lifetime and quantum yield of the Pt(diimine)(dithiolate) chromophore. The lifetimes and quantum yields of emission in dichloromethane at 298 K are presented in Table 2 for the two series of complexes. The Pt(diimine)(dithiolate) complexes display lifetimes ranging from 1 ns to over 1 μs and Φ_{em} ranging from $<10^{-5}$ up to 6.4×10^{-3} , indicating that the nature of the ligands has a large influence on the kinetics of excited-state decay. The complexes having toluenedithiolate have lifetimes that are significantly longer than those measured previously for other Pt(diimine)(dithiolate) complexes.

An analysis of the decay rates shows that two trends are evident for the Pt(diimine)(tdt) series. Nonradiative decay rate constants increase, while radiative decay rate constants decrease in going from complex **6** to **13**. These two effects can be understood in terms of the Energy Gap Law and the Einstein equation for spontaneous emission, respectively.

The Energy Gap Law predicts that the rates of nonradiative decay increase when the energy gap separating the ground and excited state decreases. The relation is based on the vibrational overlap between the ground and excited state, and k_{nr} is a function of a vibrationally-induced electronic coupling term and a Franck–Condon overlap integral. For a set of chromophores having excited states with a similar orbital basis and vibrational coupling, a simplified form of the Energy Gap Law is obtained that predicts a linear relation between $\ln(k_{\text{nr}})$ and E_{em} . This correlation has been observed for the nonradiative decay rates of the MLCT excited states of (1) complexes of the type $\text{M}(\text{diimine})_n(\text{LL})_{3-n}^{2+}$ ($\text{M} = \text{Os}, \text{Ru}; n = 1, 2$),^{43,53–56} and Re-

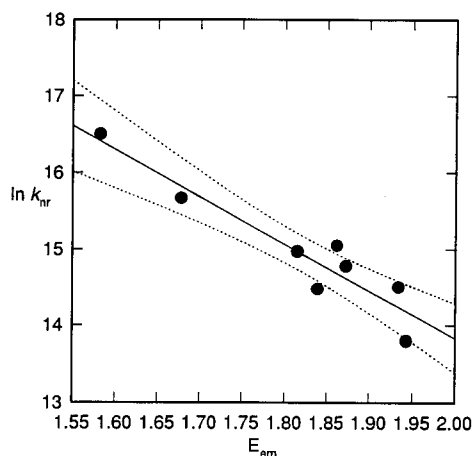


Figure 8. Plot of $\ln(k_{\text{nr}})$ vs. E_{em} (77 K, butyronitrile) for Pt(diimine)(tdt) complexes **6–13** with a linear least-squares fit to the data and 95% confidence limits.

(bpy)(CO)₃L⁺,⁵⁷ where the energy gap is tuned by variation in the nonchromophoric ligand L, (2) complexes of the type $\text{Os}(\text{NN})_n(\text{LL})_{3-n}^{2+}$ ($n = 0–3$)⁵⁸ and $\text{Ru}(\text{NN})_3^{2+}$ ⁵⁹ where the energy gap is tuned by variation in the chromophoric diimine ligand NN, and (3) $\text{Ru}(\text{bpy})_3^{2+}$ ⁶⁰ and $\text{Os}(\text{phen})_3^{2+}$ ⁶¹ for which the energy gap is tuned by variations in the solvent and counter ion, respectively. The most quantitative application of the Energy Gap Law has been presented by Meyer *et al.* for a series of Os(II) polypyridyl complexes.⁵⁷ Application of the Energy Gap Law to Pt(II) chromophores has received almost no attention. Che has proposed that solvent effects on k_{nr} observed for Pt(5-Ph-phen)(CN)₂ follow the Energy Gap Law, but the effects are small, and it is not clear that the energy gap is the significant influence on k_{nr} .¹³

The energy gap for complexes **1–13** have been approximated using the low-temperature emission maxima. The plot of $\ln(k_{\text{nr}})$ vs E_{em} for complexes **6–13** given in Figure 8 shows a good qualitative agreement with the Energy Gap Law. This is the first example of successful application of the law to a Pt(II) chromophore. The slope of -6.2 eV^{-1} is similar in magnitude to those found for Os(II) and Ru(II) diimine complexes. This correlation suggests that the charge-transfer-to-diimine excited states of the complexes **6–13** all have very similar vibrational and electronic components. Deviation from a linear relation between $\ln(k_{\text{nr}})$ and E_{em} would occur for a series of complexes in which the vibrational modes of deactivation and the electronic structure differ significantly. For many transition metal diimine complexes, the dominant acceptor vibration has been attributed to a ring stretching mode of $\sim 1300 \text{ cm}^{-1}$, which is determined from the observed progression in the structure of the 77 K emission profile.^{53,54,60,62} No vibrational progression is resolved in the 77 K emission spectra for complexes **6–13**, but the bandshapes are very similar in shape, suggesting similar vibrational components. In general, larger deviation from linearity is observed when chromophoric ligands are varied than

(55) Kober, E. M.; Marshall, J. L.; Dressick, W. J.; Sullivan, B. P.; Caspar, J. V.; Meyer, T. J. *Inorg. Chem.* **1985**, *24*, 2155–2163.

(56) Kalyanasundaram, K.; Nazeeruddin, M. K. *Chem. Phys. Lett.* **1992**, *193*, 292–297.

(57) Caspar, J. V.; Meyer, T. J. *J. Phys. Chem.* **1983**, *87*, 952–957.

(58) Johnson, S. R.; Westmoreland, T. D.; Caspar, J. V.; Barqawi, K. R.; Meyer, T. J. *Inorg. Chem.* **1988**, *27*, 3195–3200.

(59) Cook, M. J.; Lewis, A. P.; McAuliffe, G. S. G.; Skarda, V.; Thomson, A. J.; Gasper, J. L.; Robbins, D. J. *J. Chem. Soc., Perkin Trans. II* **1984**, 1293–1311.

(60) Caspar, J. V.; Meyer, T. J. *J. Am. Chem. Soc.* **1983**, *105*, 5583–5590.

(61) Meyer, T. J. *Pure Appl. Chem.* **1986**, *58*, 1193.

(62) Crosby, G. A. *Acc. Chem. Res.* **1975**, *8*, 231.

(52) Wayne, R. P. *Principles and Applications of Photochemistry*; Oxford University Press: Oxford, 1988.

(53) Caspar, J. V.; Kober, E. M.; Sullivan, B. P.; Meyer, T. J. *J. Am. Chem. Soc.* **1982**, *104*, 630–632.

(54) Kober, E. M.; Caspar, J. V.; Lumpkin, R. S.; Meyer, T. J. *J. Phys. Chem.* **1986**, *90*, 3722–3734.

when nonchromophoric ligands are varied because nonradiative decay is sensitive to vibrations localized on chromophoric ligands. Specific differences have been observed between two series of Os(diimine)₂(LL) complexes for which diimine = bpy and phen.^{53,57} Energy Gap Law correlations for the two series yield parallel lines with different intercepts, and the bpy complexes have k_{nr} values ~ 3 times those of the phen analogs. A similar result is found in this study, in which k_{nr} for Pt(bpy)-(tdt) (**12**) is approximately twice that of Pt(phen)(tdt) (**11**).

In contrast, there appears to be no correlation between $\ln(k_{nr})$ and E_{em} for the series of Pt(dbbpy)(dithiolate) complexes (**1–5** and **7**), suggesting that factors in addition to the energy gap are important to the nonradiative decay pathways for this series of complexes. Whereas the Pt(diimine)(tdt) complexes vary only by the substituents on the bipyridine or phenanthroline backbone, the Pt(dbbpy)(dithiolate) complexes differ a great deal in the structure of the dithiolate, varying between four- and five-membered chelate rings as well as in functional groups on the dithiolate backbone.

The series of Pt(dbbpy)(dithiolate) complexes may also differ in their electronic structure as a result of additional low-lying excited states of different orbital parentage. Deactivation via low-lying metal-centered (MC) d–d states has been an important consideration for transition metal diimine complexes. The influence of MC excited states on the photoluminescence of several Pt(II) chromophores has been reported.^{10,63} The energies of ³MC transitions for Pt(II) complexes have been estimated to be $\sim 17\,000\text{ cm}^{-1}$ for Pt(NH₃)₂Cl₂, $\sim 22\,000\text{ cm}^{-1}$ for Pt(bpy)-(ethylenediamine), and $\sim 23\,000\text{ cm}^{-1}$ for Pt(bpy)Cl₂.⁶³ No unambiguous assignment of MC transitions has been made for the Pt(diimine)(dithiolate) chromophore. For complexes such as **1** and **2**, which have CT emitting states at higher energy, deactivation by energetically-close MC states may be an efficient process. The presence of low-lying charge-transfer-to-dithiolate excited states has been proposed for some Pt(diimine)(mnt) complexes and may provide additional pathways for nonradiative decay.²⁰ The higher-energy emission from the Pt(dbbpy)-(dithiolate) complexes makes these additional excited states, which possess vibrational modes and electronic structure that are different from the charge-transfer-to-diimine emitting state, important for understanding why variation in the dithiolate leads to changes in the emission lifetime that do not correlate with the Energy Gap Law.

The second component of the lifetime is the radiative decay rate constant, k_r . Although the effect is smaller than the changes observed in k_{nr} , there is a systematic decrease in k_r through the series of complexes **1–13**. The Einstein equation for spontaneous emission predicts that, for a series of related excited states, k_r scales with E_{em}^3 , assuming that the electronic transition moment integral remains constant. For the complexes **1–13**, k_r increases with E_{em}^3 but a plot of the correlation exhibits curvature (Figure 9). Differences in the molar extinction coefficients of the complexes indicate that the transition moment integral is not constant for the ¹CT transition, but information regarding the transition moment integral involving the ³CT emitting state is unclear. Although the importance of k_r on the emission lifetimes increases at higher energies, for complexes in the present study, the lifetimes of those systems having the highest E_{em} are still most strongly influenced by k_{nr} rather than k_r .

Tuning the Thermodynamics of Electron Transfer from the Excited State. We have recently reported estimations of excited-state reduction potentials, $E(\text{Pt}^{*/-})$ for several Pt-(diimine)(dithiolate) complexes. Values were calculated using

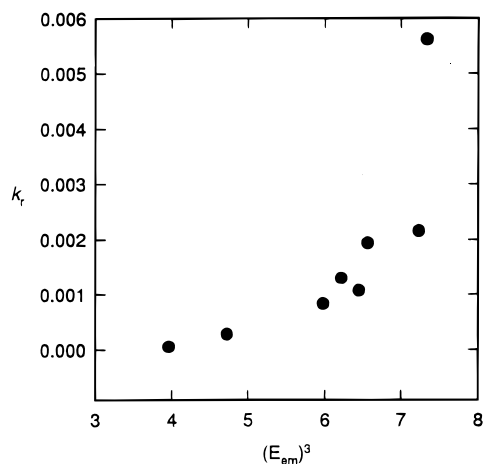


Figure 9. Plot of k_r vs. E_{em}^3 (77 K, butyronitrile) for Pt(diimine)(tdt) complexes **6–13**.

eq 4a, and a Rehm–Weller analysis of electron-transfer quenching data for one complex gave a similar value. The resulting $E(\text{Pt}^{*/-})$ values ranged from 0.96–1.15 V (vs SCE) for six compounds prepared from combinations of four different dithiolates with two different diimines, but no trend was evident.

The excited-state reduction potentials for the complexes in this study show two trends. For the Pt(dbbpy)(dithiolate) series of complexes **1–5** and **7**, $E(\text{Pt}^{*/-})$ values decrease from 1.21 V for Pt(dbbpy)(tbcda) (**1**) to 0.54 V for Pt(dbbpy)(tdt) (**7**). This trend reflects the fact that the ground-state reduction potentials change very little with variations in the dithiolate, which is consistent with a diimine-localized reduction, while the E_{em} values for the series decrease substantially, thus leading to the large difference in $E(\text{Pt}^{*/-})$. For the series of Pt(diimine)(tdt) complexes **6–13**, both the ground-state reduction potential and E_{em} decrease as the diimine becomes more electron-withdrawing, so changes in $E(\text{Pt}^{*/-})$ are much smaller, with a range of only 0.18 V. The excited-state oxidation potentials show the opposite trend for both series. The Pt(dbbpy)(dithiolate) series of complexes **1–5** and **7** possess a small range of $E(\text{Pt}^{+/*})$ values, with the exception of complex **5**. In contrast, the Pt(diimine)-(tdt) series of complexes **6–13** possess a large range of $E(\text{Pt}^{+/*})$ values.

Because the excited-state redox potentials for the Pt(diimine)-(dithiolate) chromophore can be systematically tuned, oxidative and reductive quenching experiments were conducted to investigate if bimolecular electron-transfer rates can be controlled in a similar manner through ligand variation. For this study, eight complexes were chosen that have desired differences in their excited-state reduction or oxidation potentials. Complexes **2**, **4**, **5**, and **7** were used for the reductive quenching experiments, since they have $E(\text{Pt}^{*/-})$ values ranging from 1.23 to 0.54 V vs NHE. For the oxidative quenching experiments, complexes **6**, **7**, **10**, and **11** were used, reflecting $E(\text{Pt}^{+/*})$ values estimated to range from -1.60 to -1.46 V vs NHE. While inclusion of Pt(EC-bpy)(tdt) (**13**) in the latter series would have increased the range, the magnitude of the lifetime and quantum yield for complex **13** is too small for sufficient quenching to be observed.

The bimolecular electron-transfer rate constants obtained from the reductive quenching experiments are given in Table 4 and range from diffusion-limited rates to rates that are too slow to observe quenching. For each complex, k_{cl} increases in going from DMA, the weakest donor, to TMPD, the strongest donor. More importantly, the rate constants increase going along the series **7** < **5** < **4** < **2** for a given electron-donor, consistent with the increases in the excited-state reduction potentials. Using DMA, the four complexes display electron-transfer rates which

range three orders of magnitude, an effect that has important implications on the design of Pt(II) chromophores for photocatalytic schemes.

The oxidative quenching experiments yielded bimolecular electron-transfer rate constants, which are given in Table 5. Each of the complexes displays increased electron-transfer rates in going from nitrobenzene to dinitrobenzene, reflecting the increased reduction potential of the oxidative quenchers. Increases in k_{el} are also observed for a given quencher when going along the series of complexes **11** < **10** < **7** < **6**. The range of values found in the oxidative quenching experiments is less than that found for the reductive quenching experiments, but this is consistent with the smaller range of excited-state oxidation potentials for the Pt(diimine)(tdt) series selected.

That the rates of electron transfer increase with the driving force of the reaction is in accord with Marcus–Hush theory, which predicts that $\ln(k_{el})$ increases with a quadratic dependence on the driving force of the reaction, ΔG_{el} .^{64,65} Through use of the Rehm–Weller equation⁶⁶ (eqs 7a and 7b) and the data from Tables 4 and 5, ΔG_{el} values were calculated where Q is the redox quencher, and W_p is a coulombic work term. For neutral metal complexes having similar shape and size and

$$\Delta G_{el} = nF[E(Q^{+/0}) - E(Pt^{*/-})] - W_p \quad (7a)$$

$$\Delta G_{el} = nF[E(Pt^{+/*}) - E(Q^{0/-})] - W_p \quad (7b)$$

neutral quenchers having similar shape and size, the work term is not expected to change significantly within the series of experiments. Plots of $RT \ln(k_{el})$ vs ΔG_{el} for the complexes **2**, **4**, **5**, **7**, **6**, **7**, **10**, and **11** were then made (see supporting information) that show a qualitative agreement with the theory's prediction. These results affirm the ability to tune the driving force of electron-transfer reactions between the Pt(II) diimine dithiolate complexes under study here and electron donors and acceptors through appropriate ligand variation.

Conclusions

The present study has shown the ability to tune important excited-state properties of the Pt(diimine)(dithiolate) chromophore by variations in molecular design. Through changes in the dithiolate and diimine ligands, the charge-transfer absorption and emission energies have been tuned by 8160 and 7400 cm^{-1} , respectively. The energies can be systematically controlled through changes in the electron donating and ac-

cepting abilities of the ligands. The influence that these changes have on the HOMO and LUMO energies supports the assignment of a charge-transfer-to-diimine excited state. The excited-state lifetimes can be tuned by 3 orders of magnitude, and many of the complexes in this study possess lifetimes in solution that are significantly longer than those of previously-studied Pt-(diimine)(dithiolate) complexes. The ability to control these lifetimes appears to depend on (1) changes in the excited-state energy, a dependence which follows the Energy Gap Law for many of the complexes, (2) changes in the structure and deactivating vibrational modes of the ligands, a dependence which is less clear to predict, and (3) the deactivation by excited states having different orbital parentage. For the development of long-lived excited states, the evidence in this work points to designing complexes with excited-state energies in the 20 000–17 000 cm^{-1} region. The empirical observations concerning the dependence of decay rates on the dithiolate indicates that complexes having tdt and dmqdt possess longer lifetimes. The ability to control the excited-state redox potential depends on the electronic effects of the dithiolate and diimine ligands. Systematic variation in the ligands can be used to tune the ground-state redox potentials and, as mentioned above, the excited-state energies in order to develop chromophores that have desired excited-state redox potentials. An additional factor in the design of the Pt(diimine)(dithiolate) chromophore that has been advanced by this work is an increase in the solubility of many of the complexes in common organic solvents. Increasing the solubility in water and designing complexes with high stability are important future developments for this chromophore.

Acknowledgment. We wish to thank the Department of Energy, Division of Chemical Sciences for support of this research. Dr. Steven Atherton is acknowledged for his assistance with single-photon counting experiments, and Dr. Brian Cleary is thanked for his help with some emission and excitation spectra. A generous loan of platinum salts from Alfa/AESAR Johnson Matthey Co. is also gratefully acknowledged.

Supporting Information Available: Plots of $RT \ln(k_{el})$ vs ΔG_{el} for reductive and oxidative quenching for complexes **2**, **4**, **5**, **7**, **6**, **7**, **10**, and **11** using data from Tables 4 and 5 (2 pages). This material is contained in many libraries on microfiche, immediately follows this article in the microfilm version of the journal, can be ordered from ACS, and can be downloaded from the Internet; see any current masthead for ordering information and Internet access instructions.

(64) Marcus, R. A. *J. Chem. Phys.* **1956**, *24*, 966.

(65) Hush, N. S. *Chem. Phys.* **1975**, *10*, 361.

(66) Rehm, D.; Weller, A. *Isr. J. Chem.* **1970**, *8*, 259.